Springer

KSME

Journal of Mechanical Science and Technology 32 (9) (2018) 4071~4078
www.springerlink.com/content/1738-494x(Print)/1976-3824(Online)
DOI 10.1007/s12206-018-0806-4

Life estimation of shafts using vibration based fatigue analysis †

Sagi Rathna Prasad and A. S. Sekhar*

Mechanical Engineering Department, Indian Institute of Technology Madras, Chennai, 600036, India

(Manuscript Received September 24, 2017; Revised May 19, 2018; Accepted June 4, 2018)

Abstract

Many rotating machinery components fail due to fatigue when subjected to continuous fluctuating stresses. Hence, estimation of fatigue crack initiation life is essential to avoid catastrophic failure. Effective vibration based fatigue life analysis requires measurement of accurate time varying signal. In this study, experimentally observed fatigue lives of rotating shaft, for three different notch configurations, are compared with fatigue lives estimated using two approaches based on an acquired vibration signal. The first one is time domain approach (based on Rainflow cycle counting) while the second one is frequency domain approach (based on power spectral density moments). In the frequency domain approach, fatigue life is estimated using the narrow-band approximation and Dirlik's empirical solution. The performance of two approaches in estimating fatigue life for the same signal length taken at different time intervals from the total signal acquired is also discussed. In addition, experimental uncertainty analysis is performed and discussed in this study. A good correlation is found between the estimated fatigue life using Dirlik's rainflow range probability density function and experimental life. Therefore, this study concludes that the Dirlik's approach can be considered as preferable method for estimating fatigue life of rotating shaft.

Keywords: Fatigue life; Palmgren miner rule; Power spectral density; Probability density function; Rainflow cycle counting

1. Introduction

The main objective in the development of modern design approach is the effective fatigue life analysis of critically stressed rotating components. Traditionally, fatigue life of a rotating shaft subjected to fully reversed bending load is obtained using S-N curves. Many factors like material properties, geometric discontinuities, loading conditions and environmental conditions etc., influence the fatigue life of a rotating component. Localized stress concentration points such as notches are usually source of early fatigue failures. Fatemi and Zeng [1] presented fatigue life predictions of circumferentially notched specimens with different stress concentration factors. A lot of research has been devoted to study the effect of notches on the fatigue failures under constant amplitude loading [1-3].

In many practical cases, rotating machinery components often undergo irregular cyclic loadings during their service life. For such kind of rotating components fatigue life can be estimated using two vibration based approaches: (i) Traditional time domain fatigue analysis which employs a technique called rainflow cycle counting method, introduced by Matsuishi and Endo [4], (ii) Spectral fatigue analysis in which stress range probability density function is constructed using spectral moments [5].

In time domain approach complex service stress history is reduced into series of half or full damaging cycles [6, 7] which can then be used to calculate their cumulative damaging effect [8]. A brief review on time domain and frequency domain fatigue analysis is presented by Halfpenny and Quigley et al. [9, 10]. Severity of damage for complex vibrations is usually described in terms of its power spectral density, PSD [11]. Many fatigue life models have been developed using first four spectral moments of stress PSD such as narrow band approximation solution [5] and Dirlik's empirical closed form solution [12]. The prediction of fatigue life using rainflow cycle counting and Dirlik's formula for cantilever beam subjected to uniaxial and multi-axial loading is presented in Refs. [13, 14]. The suitability of time and frequency domain approaches for different mechanical components and their relative advantages and disadvantages is presented by Rao [15]. Fatigue life estimated using rainflow cycle counting and Dirlik's approach for data measured from various locations of wind turbine is presented by Regan [16]. In all the above mentioned references, fatigue life is calculated by employing various spectral methods for numerically simulated or real machine/structural vibration data and is compared with estimated life using time domain method. But to ascertain the accuracy of both time and frequency domain methods, it is required to compare the estimated fatigue life with life obtained from experiments.

*Corresponding author. Tel.: +91 44 22574709, Fax.: +91 44 2257 4652
E-mail address: as_sekhar@iitm.ac.in
† Recommended by Associate Editor Jun-Sik Kim

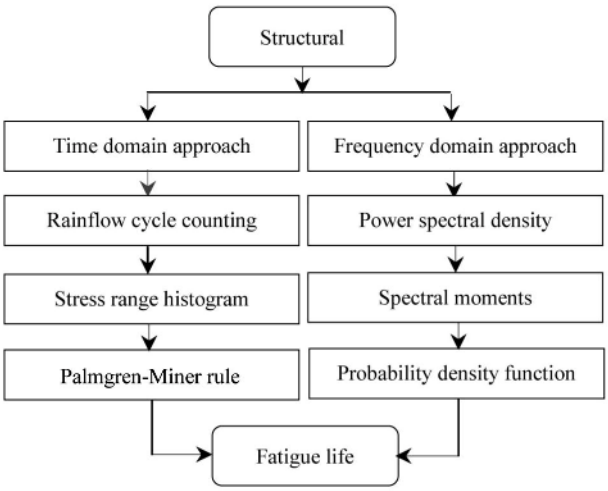

Fig. 1. Flow chart for fatigue life estimation.

The usefulness of Dirlik's method in estimating fatigue life of different dynamic structures like offshore platforms, cantilever beams and automotive frames etc., is demonstrated in the previous studies. However, no detailed studies have been conducted to estimate the fatigue of life rotating shafts undergoing irregular loads using both time and frequency domain methods. Simple rotating shafts subjected to constant static bending load exhibit predominantly periodic responses due to residual unbalance. However, the undetermined inaccuracies in rotor bearing system like unbalance, misalignment, shaft bend and the surface imperfections in bearing housings etc., results in irregular random vibration response [17]. For such shafts prediction of fatigue life using S-N curves is not appropriate and has to be replaced with more advanced methods.

In the present study, experimental fatigue life of a notched rotating shaft is compared with estimated life using traditional S-N curve, time domain and spectral domain methods. The performance of selected methods for same signal length taken at different intervals from the total acquired signal until the final failure of each specimen is studied. Finally, experimental uncertainty analysis is performed and discussed.

2. Theoretical background of fatigue life theories

The general procedure to estimate the fatigue life has been given in a flow chart as shown in Fig. 1.

2.1 Time domain approach

Response in time domain measured from typical rotating machinery is mostly irregular. Rainflow cycle counting method [8, 18], a standard tool for fatigue life prediction models, decompose irregular time history into an equivalent sets of stress blocks [19]. The number of cycles obtained in each block is stored in a stress range histogram. Further a linear damage accumulation (Palmgren-Miner) rule in conjunction with material life (S-N) curve is used to estimate the fatigue life. The combination of rainflow cycle counting method and Palmgren-Miner rule, tested extensively, is commonly accepted for fatigue life analysis. In general Palmgren-Miner rule states damage fraction, D (= n/N) for a given stress range (S). Failure is assumed to occur when accumulated damage, D, equals unity. Here n is the number of cycles accumulated for the stress range (S) and N is the number of cycles to failure at the same stress range (S) calculated from Wohler's (S-N Curve) equation, expressed as shown in Eq. (1). In this equation m is the slope of the S-N curve and 'a' is the material parameter determined by experiments.

$$NS^m = a\,. \tag{1}$$

2.2 Frequency domain approach

General procedure for frequency domain fatigue calculation is shown in Fig. 1. Unlike time domain approach, stress response obtained from rotating machinery is described using conventional statistical function called power spectral density (PSD). Once the PSD plot of a rotating component is achieved then the terms needed for fatigue life estimation methods are calculated from first four moments of a one sided PSD [20]. Stress range probability density functions (PDF) are constructed using the first four moments of PSD, which provides equivalent information as obtained from rainflow cycle counting method. If a probability density function of rainflow ranges is attained, then fatigue life is estimated using material S-N curve equation. The n^{th} moments of one sided PSD are calculated using following equation

$$m_n = \int_0^\infty f^n G(f)\,df = \sum f_k^n G_k(f)\,\Delta f \tag{2}$$

where G_k (f) describes the amount of average power contained in a frequency band. The area under PSD represents mean square amplitude of the signal and square root of this is equal to standard deviation for zero mean time history. Irregular stress time histories can be characterised using statistical parameters like expected number of upward zero-crossings per second (E[0]) and expected number of peaks per second (E[P]) in the signal. The ratio of (E[0]/E[P]) is called irregularity factor (γ). These relations as given in Eq. (3) are imperative for determining fatigue life. These are defined in terms of spectral moments as

$$E[0] = \sqrt{\frac{m_2}{m_0}}; \quad E[P] = \sqrt{\frac{m_4}{m_2}}; \quad \gamma = \frac{E[0]}{E[P]}. \tag{3}$$

2.2.1 Narrow band method

A remarkable step towards estimating fatigue life from PSD's was attempted by Bendat [5]. This method assumes that the PDF of peaks is equal to the PDF of stress ranges. The expression for probability density function and expected cu-

mulative damage per unit time, E[D], of narrow band PSD is given as,

$$p_{NB}(S)=\left[\frac{S}{4m_0}e^{\frac{-S^2}{8m_0}}\right];\ E[D]=\frac{E[P]}{a}\int S^m p_{NB}(S)dS \tag{4}$$

where E[P] is expected number of peaks, S is the stress range, m_0 is the area under PSD, 'a' and 'm' are the material constants obtained from S-N curve. Fatigue life in seconds is obtained by equating Eq. (4) to unity.

2.2.2 Dirlik's empirical solution

Dirlik [12] obtained empirical closed form solutions for the PDF of ordinary and rainflow ranges for estimating fatigue life directly from a wide band PSD of stress. This was achieved using computer simulations to model the signals using Monte Carlo technique. Ordinary range counting technique identifies and records the height of ranges between successive peaks and troughs. Whereas, rainflow range counting technique determines cycles associated with closed stress hysteresis loops formed from different parts of the signal. The Dirlik's expression for ordinary ranges is

$$p_{OR}(S)=\frac{\frac{C_1}{\tau}e^{\frac{-Z}{\tau}}+\frac{C_2 Z}{\alpha^2}e^{\frac{-Z^2}{2\alpha^2}}}{2\sqrt{m_0}} \tag{5}$$

where the function parameters are defined as:

$$C_1=\frac{X_m-X_{\min}}{\gamma^2};\tau=0.02+\frac{2(X_m-X_{\min})}{\gamma};C_2=1-C_1$$

$$X_m=\frac{m_1}{m_0}\sqrt{\frac{m_2}{m_4}};X_{\min}=\frac{\gamma(1+\gamma^2)}{2}.$$

The Dirlik's expression for rainflow ranges is

$$p_{RR}(S)=\frac{\frac{D_1}{Q}e^{\frac{-Z}{Q}}+\frac{D_2 Z}{R^2}e^{\frac{-Z^2}{2R^2}}+D_3 Z e^{\frac{-Z^2}{2}}}{2\sqrt{m_0}} \tag{6}$$

where the function parameters are defined as:

$$Z=\frac{S}{2\sqrt{m_0}};D_1=\frac{2(X_m-\gamma^2)}{(1+\gamma^2)};X_m=\frac{m_1}{m_0}\sqrt{\frac{m_2}{m_4}};D_2=\frac{1-\gamma-D_1+D_1^2}{1-R}$$

$$D_3=1-D_1-D_2;R=\frac{\gamma-X_m-D_1^2}{1-\gamma-D_1+D_1^2};Q=\frac{1.25(\gamma-D_3-D_2R)}{D_1}$$

where Z is the normalized stress range (S), X_m is the mean frequency of the signal and (γ) is the irregularity factor.

The expected fatigue damage per unit time is calculated as

Table 1. Notch geometric and fatigue design properties.

Property	Specimen-1	Specimen-2	Specimen-3
Notch depth (mm)	1.000	1.250	1.500
% of notch depth	6.250	7.812	9.375
Notch width (mm)	1.500	1.800	2.000
Geometric stress concentration factor (K_t)	6.944	7.375	7.780
Notch sensitivity factor (q)	0.167	0.167	0.167
Fatigue stress concentration factor (K_f)	1.995	2.068	2.136
Slope of S-N curve (m)	3.382	3.304	3.288
Material parameter (a)	8.30×10^{31}	1.80×10^{31}	1.34×10^{31}

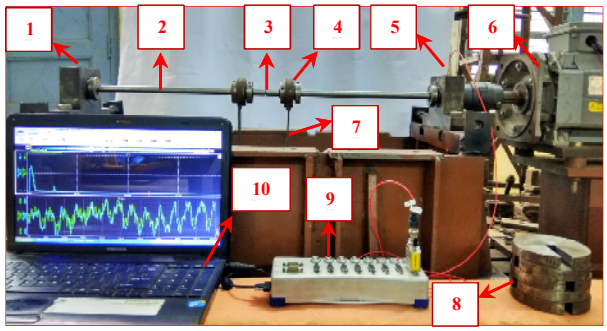

Fig. 2. Experimental rotor test rig: (1) Bearing, (2) shaft, (3) notch location, (4) auxiliary bearing, (5) accelerometer, (6) motor, (7) weight hanger, (8) dead weights, (9) DAQ, (10) computer.

$$E[D]=E[P]\int_0^\infty \frac{1}{N(S)}p_{RR/OR}(S)dS \tag{7}$$

where N(S) is the relation between the number of loading cycles to failure at stress range(S) is given in Eq. (1). Expected fatigue life in seconds can be obtained by equating Eq. (7) to unity.

3. Experimental details

A rotor test rig, shown in Fig. 2, is designed and developed according to the function specification proposed by ASTM E468-11 standard. A shaft (AISI 1020 Bright Steel) of diameter 0.016 m and length 1m is mounted on two main bearings as shown in Fig. 2. All the bearings used are self-sealed spherical roller types which have high load carrying capacity. A combination of weight hanger and slotted dead weights are used to apply the static load on the shaft through two auxiliary load carrying bearings (see Fig. 2).

Circumferential V-notch is seeded at the designated location on the shaft as per ASTM fatigue testing manual-1949. Geometrical properties of V-notch fabricated with same notch root radius of 0.02 m and notch opening angle 60 degree, on three shafts are presented in Table 1. The geometric stress concentration factor (K_t), fatigue stress concentration factor (K_f) and

notch sensitivity factor (q) are calculated using equations presented in Refs. [21, 22]. Considering high cycle fatigue region ($10^3 < N < 10^6$) the slope of S-N curve (m) and material parameter (a) calculated using Eq. (1) are presented in Table 1.

4. Results and discussion

4.1 Experimental results

Prior to the fatigue life test of each specimen, an experimental modal analysis was performed to infer the natural frequencies of the rotor bearing system. First three natural frequencies are estimated as 25 Hz, 184 Hz and 475 Hz. In all the three tests, the motor was set to spin at 1035 rpm (17.25 Hz) with each specimen carrying a dead weight of 110 N. Experiments are conducted till the final failure of each specimen. A sudden rise in statistical parameters like root-mean square (RMS), kurtosis and crest factor of the acquired vibration signal are observed near the final failure of each specimen. This stage is considered as a fatigue crack initiation of specimen. Experimentally obtained fatigue crack initiation lives of three specimens along with calculated life using S-N equation are presented in Table 2. The number of cycles to failure obtained using S-N curve is divided by 17.25 Hz to get life in seconds.

4.2 Theoretical results

Data acquisition system (Dewe-43 V) is used to record the response obtained from a miniature accelerometer. This has sensitivity 100 mv/g, range 50 g and is mounted on bearing housing as shown in Fig. 2. A sampling frequency of 20 KHz is chosen in order to ensure that the errors in identifying alternating peaks and troughs are minimized to a negligible level. The synchronous vibration data are acquired using two accelerometers of same specifications for initial 100 seconds of each fatigue test. One accelerometer is mounted on the bearing housing and the other is mounted on the auxiliary bearing. Due to safety reasons accelerometer on the auxiliary bearing is not mounted till the final failure of the specimen. As expected the RMS value for the data corresponding to auxiliary bearing is higher than that of bearing housing data. Based on these values, a transmissibility factor is determined as ratio of RMS value of the auxiliary bearing data (1.773) to the RMS value of the bearing housing data (0.0464). The acceleration time data acquired from the bearing housing is multiplied by the transmissibility ratio (38.2), to estimate acceleration data at the auxiliary bearing location. The FFTs of the measured acceleration data at the auxiliary bearing and estimated acceleration data after using transmissibility ratio on the bearing housing data are compared in Fig. 3. It is observed that the FFTs of both the data produce same frequency components with almost similar amplitudes. Thus the estimated acceleration data at the auxiliary bearing (close to the critical location of the shaft) are used for further study. Then the noise in the acceleration signal is eliminated using wavelet based denoising technique.

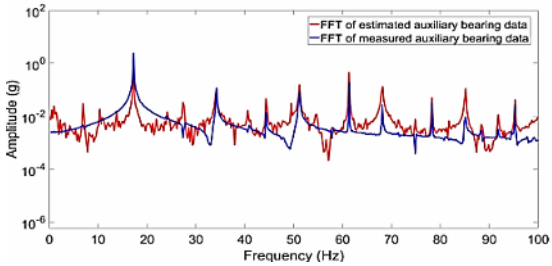

Fig. 3. FFT of estimated and measured auxiliary bearing data.

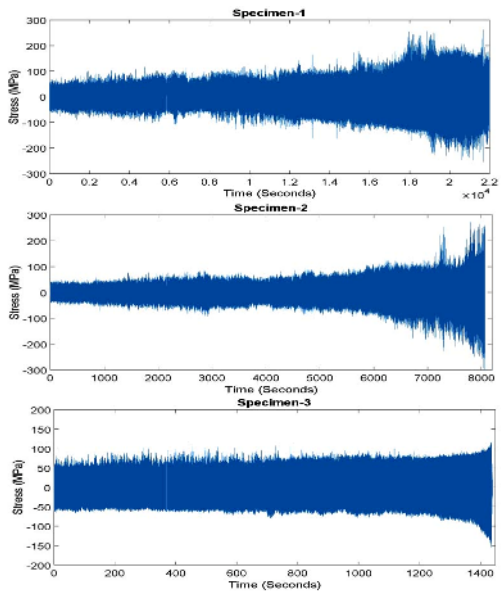

Fig. 4. Entire fatigue stress time history of three specimens.

Further, the estimated acceleration data is converted to stress signal by using symmetric static loading conditions on the shaft. Therefore, the approximate dynamic stress close to the critical location of shat is calculated using Eq. (8).

$$\sigma_b(t) = \left[\frac{16ml}{\pi D^3}\right]\left(\frac{N\sec^2}{m^3}\right)A(t)\left(1g = 9.803\frac{m}{s^2}\right) \tag{8}$$

where (σ_b) is the bending stress, D = diameter of the shaft, l = distance between main and load bearings (0.44 m) and 'm' is the total mass which including mass of shaft, hanger and dead weights (11.2 Kg). A (t) is the estimated auxiliary bearing acceleration data in g units.

The same analysis is performed for obtaining stress time history of each specimen. The entire fatigue stress time history of the three specimens is shown in Fig. 4.

4.2.1 Time domain analysis

The initial 1200 seconds stress time history of specimen-2 is used for fatigue life analysis. As per the procedure discussed in Sec. 2.1, rainflow cycle counting is performed using MATLAB toolbox developed based on ASTM E-1049 stan-

Table 2. Experimental and estimated fatigue life using time domain method and S-N curve equation.

Test specimen	Experimental test life (seconds)	Time domain life (seconds)	Relative error %	Life calculated using S-N Curve equation in seconds
1	21800	26967	23	29834
2	8423	10245	22	24075
3	1419	1973	39	21828

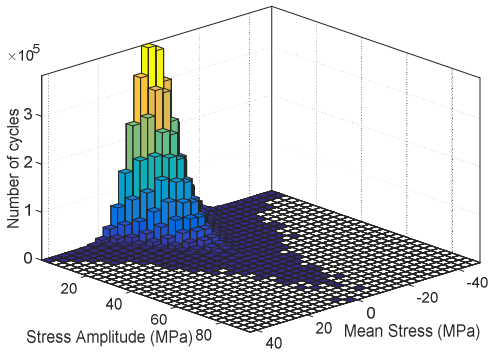

Fig. 5. Rainflow matrix of test specimen-2.

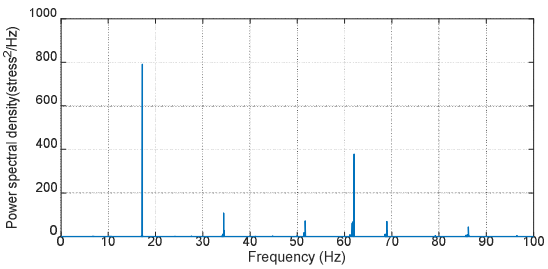

Fig. 6. Power spectral density of stress time history.

dard [23]. Each cycle in rainflow flow matrix obtained, shown in Fig. 5, contributes to certain amount of fatigue damage. The total accumulated damage using Palmgren-Miner rule and Eq. (1) is obtained as 0.11713.

The expected fatigue life of the component is calculated as ratio of length of time history (1200 seconds) to the accumulated damage (0.11713). Thus the expected fatigue of the test specimen-2 is obtained as 10245 seconds. Using similar procedure the expected fatigue life for test specimen-1 and test specimen-3 are obtained and presented in Table 2. The relative error in these estimated values with respect to experimental life is calculated and is also shown in Table 2.

4.2.2 Frequency domain analysis

As discussed in Sec. 2.2, spectral fatigue analysis is carried out on same stress time history used in time domain analysis. Power spectral density (PSD) is computed and plotted for a frequency range of 0 to 100Hz is shown in Fig. 6.

From PSD, the values of first four moments and other significant statistical parameters calculated using Eqs. (2) and (3), are: $m_0 = 115$, $m_1 = 3.45\times10^5$, $m_2 = 1.85\times10^9$, $m_4 = 9.12\times10^{16}$, $E[P] = 7.02\times10^3$, $E[0] = 4.01\times10^3$ and $\gamma = 0.5713$.

Table 3. Estimated fatigue life using narrow band (NB), Dirlik's ordinary range (OR) and Dirlik's rainflow range (RR).

Test Sp.	Exp. test life (seconds)	Estimated life in seconds			Relative error %		
		NB	OR	RR	NB	OR	RR
1	21800	2196	36188	24131	90	66	11
2	8423	1556	14319	9421	81	70	14
3	1419	932	1802	1589	34	27	12

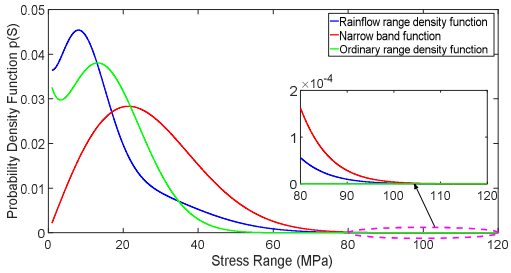

Fig. 7. Narrow band and Dirlik's probability density functions.

Using these values narrow band, ordinary and rainflow range probability density functions are computed using Eqs. (4)-(6) and are plotted as shown in Fig. 7. Expected fatigue life of test specimen-2 using Eqs. (4) and (7) is presented in Table 3. A similar procedure for test specimen-1 and test specimen-3 is carried out, corresponding results are also presented in Table 3. The relative error in the estimated values with respect to experimental life is also calculated and is shown in Table 3.

4.3 Experimental uncertainty analysis

The following parameters are considered for uncertainty analysis.

4.3.1Effect of installation irregularities and operating conditions in the rotor bearing system

In general, any irregularities that occurred during the installation of test rig for each experiment are often reflected by changes in the vibration pattern measured in operational condition. The uncertainty in the test rig is analyzed by considering initial 300 seconds of measured vibration data from each experiment. For the first few minutes, although the specimens are having different notch sizes, the vibration data are expected to be same. As the amount of irregularities is manifested in the frequency spectra, fast Fourier transform (FFT) is computed for each data and plotted for a frequency range of 0 to 100 Hz as shown in Fig. 8.

The harmonics of operating speed (17.25Hz) observed in Fig. 8 reflect the different types/combination of irregularities in the test rig. From Fig. 8 it can be concluded that the operating conditions of three experiments and irregularities in the test rig are similar in all the three experiments. The percentage deviations of amplitudes at each frequency component are calculated. The maximum deviation is observed in the operat-

Table 4. Fatigue life estimated at different time intervals for the raw and denoised signal.

Specimen-2 vibration data considered at different intervals in minutes						
Method	Noise signal/raw signal			Denoised signal		
	0-20	40-60	100-120	0-20	40-60	100-120
RF (seconds)	15621	18426	21012	10245	10621	9990
DRR (seconds)	14289	16743	19647	9421	9381	9289

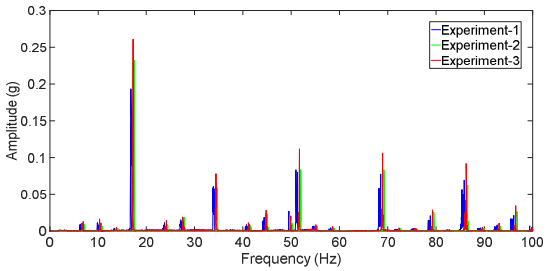

Fig. 8. FFT of acceleration time history.

ing frequency component and it is less than 4 %, whereas, deviations in higher harmonics like 2X to 5X are less than 2 %. Thus, the uncertainty analysis of the experiments indicates vibration data acquired for fatigue life analysis are under the same experimental conditions.

4.3.2 The effect of noise in the measured data

Vibration data measured using transducer like accelerometer is always corrupted by noise and results in some random error. To understand this effect, complete experimental data for specimen-2 is considered. Fatigue life is estimated for same length of noisy signal at different intervals and is compared with estimated fatigue life of denoised signal. Time domain based rainflow range counting method (RF) and Dirlik's rainflow range probability density function (DRR) are used to estimate the fatigue life. The estimated fatigue lives are presented in Table 4. It is noticed that the fatigue life analysis is over sensitive to the noise in the measured data. Whereas, the denoised signal results are closer to the experimental value of 8423 seconds. Thus, for the effective fatigue life analysis noise content has to be removed without the loss of true structural vibration data.

4.3.3 Uncertainty in estimating fatigue life using rainflow counting method and Dirlik's rainflow range probability density function

Random error associated with two methods in estimating fatigue life is studied and is discussed in this section. Rainflow cycle counting method applied directly on a time signal requires accurate measurement of peaks and troughs. With high sampling frequency (50 times greater than maximum frequency of interest) variation of the acquired stress signal is complex due to unwanted frequency components in it. Therefore, it is difficult to detect all peaks and troughs that form a cycle which results in the possible errors. Thus, the fatigue life estimated using finite length of the signal taken at different time instants will show scatter [24]. Whereas, in the Dirlik's rainflow range method the effect of stresses contained in the total frequency range is considered for evaluating fatigue life. Thus, Dirlik's rainflow range method depends upon the power spectral density of the signal. However, a similar scatter in the estimated fatigue life is observed using Dirlik's rainflow range method due to variance error and biased error in estimating power spectral density [25]. During data acquisition process, it is observed that the variation of the signal is arbitrary at different time instants. Thus, the fatigue life evaluated using these methods at different time instants will show scatter.

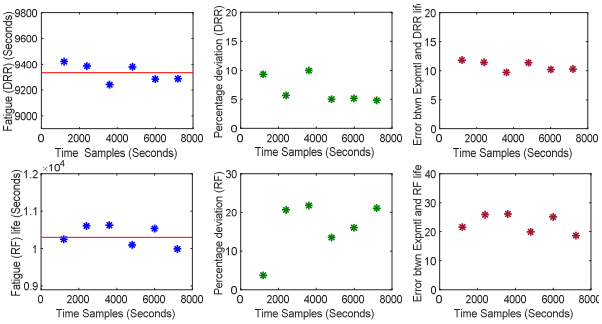

Fig. 9. Estimated fatigue life, percentage deviation and absolute error of each time sample of specimen-2.

This analysis is performed by considered full experimental data of specimen-2 as shown in Fig. 4. Time samples of same length (1200 seconds) taken at successive intervals throughout the entire length of acquired signal. Fatigue life is estimated for each time sample using two methods is plotted and shown in Fig. 9.

In Fig. 9, the first column of plots represents the estimated fatigue life at each successive interval using Dirlik's rainflow range method (DRR) and rainflow cycle counting method (RF). The red line in those plots indicates mean value of estimated fatigue life of all time samples. The second column of plots in Fig. 9 represents the percentage deviation of estimated fatigue life for each sample from the mean value, thus indicates precision of the method. The third column in Fig. 9 shows the absolute error between estimated fatigue life for each sample and experimental fatigue which indicates the accuracy of the method. From Fig. 9, it is observed that the precision and accuracy of Dirlik's method is more significant than rainflow cycle counting method. Identical results are observed when the same analysis is performed for other two specimens. Therefore, the uncertainty in estimating fatigue life using Dirlik's method is less than rainflow range method.

4.4 Discussion

From Table 2, fatigue life obtained using S-N curve equation is falsifying when compared with experimental fatigue

life. Therefore, predicting fatigue life of rotating shafts, operating under these kind of experimental conditions, using S-N curve is inappropriate. Hence, vibration based approaches like time and frequency domain methods can be examined to estimate fatigue life. From Table 3, it is found that the narrow band method underestimates and Dirlik's ordinary range method overestimates the fatigue life. Also from Table 3, it is observed that the narrow band method is so conservative due to ignoring positive troughs and negative peaks of the signal. And also, by assuming all positive peaks are paired with corresponding troughs of similar magnitude on the other side of the mean regardless whether they actually form stress cycles [11]. This is the reason the narrow band has a higher probability density at all high stress ranges and can be seen in inset figure of Fig. 7. From Fig. 7, it is also noticed that the probability density of rainflow range is considerably higher at low stress ranges when compared to probability density of ordinary ranges. This is due to rainflow range technique initially extracts small range cycles leaving the larger cycles to be counted later. And also it is noticed that the rainflow range probability density is slightly higher at high stress ranges when compared to probability density of ordinary ranges (see inset figure of Fig. 1). This is vital because it is these extra cycles which cause significant difference in estimating the fatigue life using Dirlik's rainflow range and ordinary range method [11]. Thus, Dirlik's rainflow range method identifies all the variations in the signal which results in estimating fatigue life with least relative error with respect to experimental fatigue life when compared with other methods (see Table 3).

From Tables 3 and 4, life estimated using rainflow counting method and Dirlik's rainflow range method is not conservative with respect to the experimental life. Over sensitiveness of rainflow cycle counting method and Dirlik's method for the noise in the measured data can be noticed from Table 4. Also from Table 4 and Fig. 9, it is noticed that the fatigue life estimated for specimen-2 using Dirlik's method for same time sample length taken at different/successive time intervals from the entire stress history excels when compared to the rainflow cycle counting method. Finally, it is noted that the precision and accuracy of Dirlik's rainflow range probability density function in estimating fatigue life is significantly higher when compared to time domain method. Therefore, Dirlik's rainflow range density function is considered as most robust and the suitable technique in predicting fatigue life of rotating shafts.

5. Conclusions

A rotor test rig is designed and developed to instigate shaft fatigue crack is reported in this paper. Fatigue tests, on three shaft specimens each seeded with different circumferential V-notch configuration, are conducted under the same experimental conditions. Vibration based fatigue life analysis of rotating shaft has been carried out in time and frequency domains. To ascertain the accuracy of time and frequency domain methods, the estimated fatigue life is compared with life obtained from experiments. Time domain approach is implemented using rainflow cycle counting MATLAB toolbox (based on ASTM E-1049 standard). Whereas fatigue life is estimated using different spectral methods such as Dirlik's rainflow range, ordinary range functions and narrow band methods. The estimated fatigue lives using S-N curve, time and frequency domains are compared with experimental fatigue life. Fatigue life obtained using S-N curve equation is falsifying when compared with experimental fatigue life. It is found that the narrow band and Dirlik's ordinary range method underestimates the fatigue life. However, it is observed that the Dirlik's probability density function of rainflow ranges outperforms (shows least error) than the other techniques used. Also, the precision and accuracy of Dirlik's PDF of rainflow ranges in estimating fatigue life is significantly higher when compared to traditional rainflow cycle counting method. Therefore, this study indicates the importance and need of using Dirlik's rainflow range density approach even in the case of rotating shafts for predicting the fatigue life.

References

[1] A. Fatemi, Z. Zeng and A. Plaseied, Fatigue behavior and life predictions of notched specimens made of QT and forged microalloyed steels, *International Journal of Fatigue*, 26 (6) (2004) 663-72.

[2] N. Daemi and G. H. Majzoob, Experimental and Theoretical investigation on notched specimen's life under bending loading, *World Academy of Science, Engineering and Technology*, 5 (2011).

[3] Q. Bader and E. Kadum, Effect of V notch shape on fatigue life in steel beam made of AISI 1037, *International Journal of Engineering Research and Applications*, 4 (6) (2014) 39-46.

[4] M. Matsuishi and T. Endo, Fatigue of metals subjected to varying stress, *Japan Society of Mechanical Engineers, Fukuoka,* Japan, 68 (2) (1968) 37-40.

[5] J. S. Bendat, Probability functions for random responses: prediction for peaks, fatigue damage, and catastrophic failures, *National Aeronautics and Space Administration, Contract Report,* 33 (1964).

[6] C. Amzallag, J. P. Gerey, J. L. Robert and J. Bahuaud, Standardization of the rainflow counting method for fatigue analysis, *International Journal of Fatigue,* 16 (4) (1994) 287-293.

[7] L. R. Gopi Reddy, L. M. Tolbert, B. Ozpineci and J. O Pinto, Rainflow algorithm-based lifetime estimation of power semiconductors in utility applications, *IEEE Transactions on Industry Applications,* 51 (4) (2015) 3368-3375.

[8] A. Fatemi and L. Yang, Cumulative fatigue damage and life prediction theories: A survey of the state of the art for homogeneous materials, *International Journal of Fatigue*, 20 (1) (1998) 9-34.

[9] A. Halfpenny, A frequency domain approach for fatigue life

estimation from finite element analysis, *Key Engineering Materials, Trans Tech Publications*, 167 (1999) 401-410.
[10] J. P Quigley, Y. L. Lee and L. Wang, Review and assessment of frequency-based fatigue damage models, *SAE International Journal of Materials and Manufacturing,* 9 (2016-01-0369) (2016) 565-577.
[11] N. W. M. Bishop and F. Sherratt, Fatigue life prediction from power spectral density data. II: Recent developments, *Environmental Engineering*, 2 (2) (1989).
[12] T. Dirlik, Application of computers in fatigue analysis, *Ph.D. Thesis*, University of Warwick (1985).
[13] S. Ariduru, Fatigue life calculation by rainflow cycle counting method, *MSME Thesis,* Middle East Technical University, Ankara, Turkey (2004).
[14] M. Yoon, K. Kim, J. E. Oh, S. B. Lee, K. Boo and H. Kim, The prediction of dynamic fatigue life of multi-axial loaded system, *Journal of Mechanical Science and Technology*, 29 (1) (2015) 79-83.
[15] J. S. Rao, Optimized life using frequency and time domain approaches, *IIUTAM Symposium on Emerging Trends in Rotor Dynamics*, Springer, Dordrecht (2011) 13-26.
[16] Regan and L. Manuel, Comparing estimates of wind turbine fatigue loads using time-domain and spectral methods, *Wind Engineering*, 3 (2) (2007) 83-99.
[17] R. Tiwari and N. S. Vyas, Stiffness estimation from random response in multi-mass rotor bearing systems, *Probabilistic Engineering Mechanics*, 13 (4) (1998) 255-268.
[18] H. Anzai and T. Endo, On-site indication of fatigue damage under complex loading, *International Journal of Fatigue*, 1 (1) (1979) 49-57.
[19] S. D. Downing and D. F. Socie, Simple rainflow counting algorithms, *International Journal of Fatigue*, 4 (1) (1982) 31-40.
[20] N. W. M. Bishop, Vibration fatigue analysis in the finite element environment, *Anales de Mecanica de la Fractura*, 16 (1999).
[21] N. A. Noda and Y. Takas, Stress concentration formulae useful for any shape of notch in a round test specimen under tension and under bending, *Fatigue and Fracture of Engineering Materials and Structures*, 22 (12) (1999) 1071-1082.
[22] B. Boardman, Fatigue resistance of steels, *ASM International, Metals Handbook,* 10 (1) (1990) 673-688.
[23] ASTM E, *Rainflow counting method*, 1049-85.2005 (1987).
[24] N. W. W. Bishop, The use of frequency domain parameters to predict structural fatigue, *Doctoral Dissertation,* University of Warwick (1988).
[25] J. S. Bendat and A. G. Piersol, *Book reviews: Engineering applications of correlation and spectral analysis*, John Wiley and sons, New York, 13 (11) (1981) 25-26.

A. Seshadri Sekhar received his Ph.D. degree from IIT Madras, India, in 1993. He is currently a Professor in the Department of Mechanical Engineering at IIT Madras. His areas of research interests are rotor dynamics, tribology, condition monitoring and vibrations. He has over 175 publications in international journals and conferences.

Sagi Rathna Prasad is currently a Ph.D. student in Department of Mechanical Engineering, IIT Madras. His research interests are in the areas of vibration based fault diagnosis and prognosis in rotating machines. His works focus on the diagnosis of fault location identification, quantification and fatigue life estimation of rotors.